CAMS Service Evolution

D5.3 Particle dry deposition 0D intercomparison

Due date of deliverable	30 June 2025
Submission date	30 June 2025
File Name	CAMAERA_D5.3_v1.1
Work Package /Task	WP5/Task 5.3
Organisation Responsible of Deliverable	HYGEOS
Author name(s)	Thierry Elias, Samuel Rémy
Revision number	1.1
Status	
Dissemination Level	PU

The CAMAERA project (grant agreement No 101134927) is funded by the European Union.
Views and opinions expressed are however those of the author(s) only and do not necessarily reflect those of the European Union or the Commission. Neither the European Union nor the granting authority can be held responsible for them.

1 Executive Summary

The objective of the CAMAERA/WP5/D5.3 deliverable is to show results of the 0D intercomparison of particle dry deposition velocity obtained from measurements and by models involved in CAMS. According to Farmer *et al.* [2021] and references therein, particle dry deposition forms the single largest model uncertainty for climate modelling. They also discuss the importance for air quality as the fine particle concentration could vary by 5 to 15% depending on the deposition scheme, and global surface accumulation mode number concentration could increase by 62% after revising a deposition model scheme.

Results from 0D deposition modules used in five regional models are presented, which are LOTOS-EUROS, GEM-AQ, MATCH, SILAM, MINNI, as well as three other models used by IFS in past cycles and candidate for future cycles. Input data were prescribed to get intercomparable results, inspiring from previous intercomparison exercises as the Air Quality Modelling Evaluation International Initiative (AQMEII) programme [Clifton *et al.*, 2023]. Furthermore a list of output parameters are delivered by the participants to compare not only the dry deposition velocity but also other “intermediary” components such as the sedimentation velocity, the efficiencies, etc, in order to comment observed differences between 0D module results. The model results are intercompared together and also with observations compiled and distributed by Pleim *et al.* [2022], made over four land use categories: evergreen needleleaf forest, deciduous broadleaf forest, grass, water.

As expected, less variability is observed for largest particles affected by sedimentation, which is satisfyingly reproduced by the 0D modules. However dry deposition is highly variable for particles smaller than 2 µm. Observed variability can be reproduced by the 0D modules when Brownian diffusion is the main contributor for particles smaller than 0.2 µm, while observations are mostly underestimated between 0.2 and 2 µm, where dry deposition depends on several processes such as the Brownian diffusion and the impaction. Only Pleim *et al.* [2022], modelled here as a potential candidate for future cycles of IFS, reproduce most measurements in this size range above forests. Above water, not only Pleim *et al.* [2022] but also the 0D deposition modules of SILAM and MINNI reproduce a significant part of the observations.

Table of Contents

2 Introduction

2.1 Background

The European Union's flagship Space programme Copernicus provides a key service to the European society, turning investments in space-infrastructure into high-quality information products. The Copernicus Atmosphere Monitoring Service (CAMS, https://atmosphere.copernicus.eu) exploits the information content of Earth-Observation data to monitor the composition of the atmosphere. Combining satellite observations with numerical modelling by means of data assimilation and inversion techniques, CAMS provides in near-real time a wealth of information to answer questions related to air quality, climate change and air pollution and its mitigation, energy, agriculture, etc. CAMS provides both global atmospheric composition products, using the Integrated Forecasting System (IFS) of ECMWF - hereafter denoted the global production system -, and regional European products, provided by an ensemble of eleven regional models - the regional production system.

The CAMS AERosol Advancement (CAMAERA) project will provide strong improvements of the aerosol modelling capabilities of the regional and global systems, on the assimilation of new sources of data, and on a better representation of secondary aerosols and their precursor gases. In this way CAMAERA will enhance the quality of key products of the CAMS service and therefore help CAMS to better respond to user needs such as air pollutant monitoring, along with the fulfilment of sustainable development goals. To achieve this purpose CAMAERA will develop prototype of new service elements of CAMS, beyond the current state-of-art. It will do so in very close collaboration with the CAMS service providers, as well as other tier-3 projects. In particular CAMAERA will complement research topics addressed in CAMEO, which focuses on the preparation for novel satellite data, improvements of the data assimilation and inversion capabilities of the CAMS production system, and the provision of uncertainty information of CAMS products.

2.2 Scope of this deliverable

2.2.1 Objectives of this deliverables

This deliverable presents intercomparison of 0D modules of particulate dry deposition, used in both regional and global models of CAMS.

2.2.2 Work performed in this deliverable

In this deliverable the work as planned in the Description of Action (DoA, WP5 T5.3) was performed.

2.2.3 Deviations and counter measures

No deviations have been encountered.

2.2.4 CAMAERA Project Partners:

HYGEOS	HYGEOS SARL
ECMWF	EUROPEAN CENTRE FOR MEDIUM-RANGE WEATHER FORECASTS
Met Norway	METEOROLOGISK INSTITUTT
RC.io	RESEARCHCONCEPTS IO
BSC	BARCELONA SUPERCOMPUTING CENTER-CENTRO NACIONAL DE SUPERCOMPUTACION
KNMI	KONINKLIJK NEDERLANDS METEOROLOGISCH INSTITUUT-KNMi
SMHI	SVERIGES METEOROLOGISKA OCH HYDROLOGISKA INSTITUT
FMI	ILMATIETEEN LAITOS
MF	METEO-FRANCE
TNO	NEDERLANDSE ORGANISATIE VOOR TOEGEPAST NATUURWETENSCHAPPELIJK ONDERZOEK TNO
INERIS	INSTITUT NATIONAL DE L ENVIRONNEMENT INDUSTRIEL ET DES RISQUES - INERIS
IOS-PIB	INSTYTUT OCHRONY SRODOWISKA - PANSTWOWY INSTYTUT BADAWCZY
FZJ	FORSCHUNGSZENTRUM JULICH GMBH
AU	AARHUS UNIVERSITET
ENEA	AGENZIA NAZIONALE PER LE NUOVE TECNOLOGIE, L'ENERGIA E LO SVILUPPO ECONOMICO SOSTENIBILE

3 Description of the particle dry deposition parameterisations

According to Farmer *et al.* [2021] and references therein, particle dry deposition forms the single largest model uncertainty for climate modelling. They also discuss the importance for air quality as the fine particle concentration could vary by 5 to 15% depending on the deposition scheme, and global surface accumulation mode number concentration could increase by 62% after revising a deposition model scheme.

This task consists in intercomparing several parameterisations of the dry deposition of particles between themselves and with observations. The main objective is to provide to the participants model with a detailed comparison of each component of their dry deposition parameterisation, and a comparison of their simulated dry deposition velocity against obsrvational datasets. A secondary objectiveis to offer a benchmark for future evolution of IFS_COMPO, the global CAMS system.

The modules are briefly described in this Section, and the comparison results are showed in next Section. In Section 5, some intermediary components of the deposition velocity are showed to explain the observed differences.

3.1 0D modules

This work focuses on 0D modules of particle dry deposition used in several models. Eight modules implemented in CAMS regional and global models are considered in this deliverable. Table 1 gives the main references they are based on. Five of these modules are used in CAMS regional models, and the three other models were, are or may be used in the future, by the global model IFS.

GEM-AQ relies on Zhang *et al.* [2001] (Z01 thereafter), which is based on Slinn [1982] for vegetated canopies. LOTOS-EUROS mostly uses Z01 except for some parameters as the particle dry deposition velocity, or the aerodynamic resistance. From the 45R1 to the 47R2 cycles, IFS-COMPO also used Z01 (labelled IFS_Z01 thereafter), and since the 47R3 cycle, IFS-COMPO is based on Zhang and He [2014] (ZH14) (IFS_ZH14).

MINNI uses the model described by Pleim and Ran [2011] (PR11). Pleim *et al.* [2022] (P22) was also implemented and evaluated in this deliverable, as a potential candidate for future CAMS developments (IFS_P22).

MATCH uses the model described by Simpson *et al.* [2012] (S12), and SILAM is based on Kouznetsov and Sofiev [2012] (KS12).

Table 1. Model list in the CAMAERA WP5 0D intercomparison exercise.

Model name	***Group***	***Main reference***	***Short ref***
LOTOS-EUROS	TNO (Netherlands)	Zhang *et al.* [2001]	Z01
GEM-AQ	IOS PIB (Poland)	Zhang *et al.* [2001]	Z01
SILAM	FMI (Finland)	Kouznetsov and Sofiev [2012]	KS12
MATCH	SMHI (Sweden)	Simpson *et al.* [2012]	S12

MINNI	ENEA (Italy)	Pleim and Ran [2011]	PR11
IFS_Z01	IFS-COMPO, 45R1-47R2 cycles	Zhang *et al.* [2001]	Z01
IFS_ZH14	IFS-COMPO, 47R3- cycles	Zhang and He [2014]	ZH14
IFS_P22	Potential candidate for future cycles	Pleim *et al.* [2022]	P22

3.2 Formulations

3.2.1 Overview of the dry deposition process parameterization

Figure 1 (from P22) illustrates the main factors of the particle dry deposition velocity (V_d), plotted in function of the particle diameter D_p. They are the Brownian efficiency (E_B) affecting the smallest particles, and both the impaction efficiency (E_{im}) and the sedimentation velocity (V_g) affecting the largest particles. Even E_{im} is strongly dependent on V_g, as it depends on the Stokes number, which is for vegetated surfaces according to Slinn [1982]:

$$St_{veg} = \frac{V_g\, u^*}{g\, A}$$

A is the characteristic radius of the collectors, u* the friction velocity and g the acceleration of gravity. Consequently two important factors of the deposition velocity are the Brownian efficiency and the sedimentation velocity, active for smallest and largest particles, respectively. They are chosen to be described in detail in this Section, and modelled values are compared in Section 5.

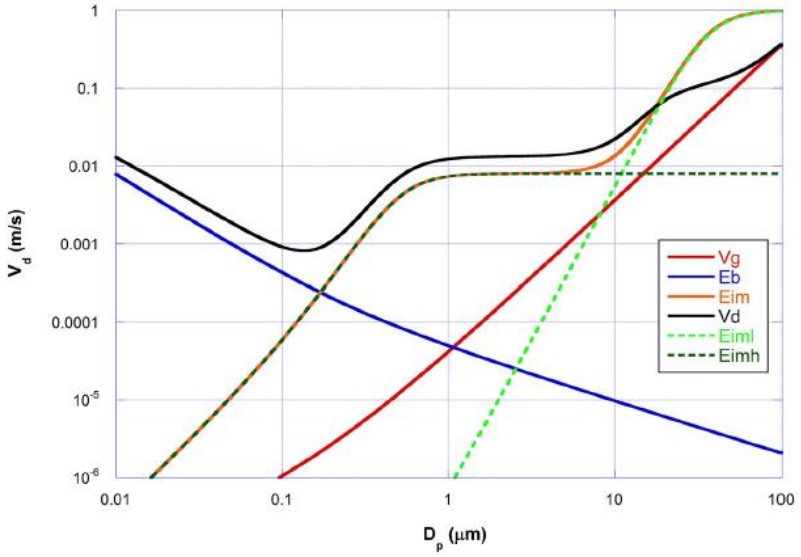

Figure 7. Size dependence of the components of the dry deposition model for needleleaf forest.

Figure 1. Main factors of the particle dry deposition velocity for needleleaf forest, from P22. Dp is the particle diameter, Eb and Eim are the Brownian and the impaction efficiencies, respectively, Eiml and Eimh are introduced by P22 as the impaction efficiencies at leaf scale and at microscale, respectively.

3.2.2 Dry deposition velocity

The formulations of the particle dry deposition velocity for the six modules implemented in GEM-AQ, LOTOS-EUROS, MINNI, IFS_Z01, IFS_ZH14, and IFS_P22, depend on the gravitational velocity V_g, the aerodynamic resistance R_a, and the surface resistance R_s. Z01 recalls the formulation of the particle dry deposition velocity given by Slinn [1982], as used by GEM-AQ , IFS_Z01, and IFS_ZH14:

$$V_d = V_g + \frac{1}{R_a + R_s} \quad (1)$$

Following Seinfeld and Pandis [2006], LOTOS-EUROS uses:

$$V_d = V_g + \frac{1}{R_a + R_s + R_a\, R_s\, V_g} \quad (2)$$

Both MINNI and IFS_P22 use the expression given by both PR11 and P22:

$$V_d = \frac{V_g}{1 - \exp(-V_g(R_a + R_b)} \quad (3)$$

R_b is named the quasi-laminar boundary layer resistance by P22. MATCH uses a similar formulation by S12 who describe EMEP, based on several authors as Weseley *et al.* [1985]:

$$V_d = \frac{V_g}{1 - \exp(-V_g(R_a + 1/V_{ds})} \quad (4)$$

The surface deposition velocity V_{ds} depends on the Monin-Obukhov length L as:

$$V_{ds} = a_1\, u^* \quad , L >= 0 \quad (5a)$$

$$a_1\, FN \left[1 + \left(\frac{-a_2}{L}\right)^{\frac{2}{3}}\right] u* \quad , L < 0 \quad (5b)$$

Where u* is the friction velocity, FN is 1 or 3 according to the compound and size range, a_2 is 300 m, and a_1 = 0.002 for all land cover categories [Weseley *et al.*, 1985] except for forest, where:

$$a_1 = 0.008\, \frac{SAI}{10} \quad (6)$$

Here, SAI=LAI+1 is the surface area index. MATCH computes the deposition velocity for two particle size ranges: PM2.5 (D_p < 2.5 µm) and PM2.5-10 (D_p > 2.5 & D_p < 10 µm).

For rough surfaces in SILAM, KS12 expresses the particle dry deposition as:

$$V_d = V_{diff} + V_{int} + V_{imp} + V_g \quad (7)$$

V_{diff} is the Brownian diffusion component, V_{int} the interception component, and V_{imp} the impaction component.

3.2.3 Sedimentation velocity

The gravitational settling (sedimentation) velocity, which "*results from a balance of gravitational and viscous drag forces as (Stokes, 1851)*" is expressed ~~by KS12 or P22 as:~~

$$V_g = \frac{g\,\rho_p\,D_p^2}{18\,\mu} C_c \quad (8)$$

Where μ is the dynamic viscosity of air (in kg s^{-1} m^{-1}), g the acceleration of gravity, ρ_p the particle density and D_p the particle diameter. C_c is "*the Cunningham slip correction factor for small particles (Cunningham, 1910)*" [P22], is named "*the correction factor for small particles*" by Z01 and is expressed as:

$$C_c = 1 + \frac{2\,\lambda}{Dp}\left(1.257 + 0.4exp\left(-\frac{0.55Dp}{\lambda}\right)\right) \quad (9)$$

Or

$$C_c = 1 + Kn\left(1.257 + 0.4exp\left(-\frac{1.1}{Kn}\right)\right) \quad (10)$$

With K_n the Knudsen number:

$$K_n = \frac{2\,\lambda}{D_p} = \frac{\lambda}{R_p} \quad (11)$$

λ is the mean free path in the air, and R_p the particle radius (D_p the particle diameter). According to Mailler *et al.* [2023], λ is given by the following empirical equation as a function of pressure P, μ and the air density ρ_a (Jennings, 1988):

$$\lambda = \sqrt{\frac{\pi}{8}} \times \frac{\frac{\mu}{0.4987445}}{\sqrt{P\rho_a}} \quad (12)$$

According to LOTOS-EUROS, the mean free path is:

$$\lambda = \frac{T}{P} 2.332e^{-5} \quad (13)$$

In GEM-AQ, the free path is calculated according to Beard (1976) as:

$$\lambda = \lambda_0 \cdot \left(\frac{\mu}{\mu_0}\right) \cdot \left(\frac{p_0}{p}\right) \cdot \left(\frac{T}{T_0}\right)^{(1/2)} \quad (14)$$

where the index “0” refers to normal-conditions values.

3.2.4 Surface, or quasi-laminar boundary layer resistance, and the Brownian efficiency

a) The surface/quasi-laminar boundary layer resistance

The five modules implemented in GEM-AQ, LOTOS-EUROS, MINNI, IFS_Z01, and IFS_P22 use the surface resistance R_s [Z01], or the quasi-laminar boundary layer resistance R_b [P22]. Both formulations of $R_{s/b}$ by Z01 and P22 are similar:

$$R_{s/b} = \frac{1}{LAI\ u*(E_B+E_{im}+E_{in})R1} \quad (15)$$

Where u* is the friction velocity, LAI the leaf area index, which is considered constant at 3 by Z01, and “*R1 is the correction factor representing the fraction of particles that stick to the surface*” [Z01]. E_b is the Brownian efficiency, E_{im} the impaction efficiency and E_{in} the interception efficiency. The formulation is slightly different for MINNI, according to PR11:

$$Rs = \frac{1}{(u* + 0.24(\frac{w*^2}{u*}))(E_B+E_{im}+E_{in})} \quad (16)$$

In this exercise, w*=0. ZH14 define the surface resistance as:

$$R_S = \frac{1}{V_{ds}} \quad (17)$$

ZH14 propose parameterisations from Z01, for three size intervals: PM2.5 (D_p < 2.5 µm), PM2.5-10, and PM10. V_{ds} is the surface deposition velocity, defined as:

$V_{ds} = a_1\ u^*$, $D_p < 2.5$ µm (18a)

$V_{ds} = (b_1\ u^* + b_2\ u^{*2} + b_3\ u^{*3})\ \exp(\ (c_1\ u^* + c_2\ u^{*2} + c_3\ u^{*3})(\frac{LAI}{LAImax} -1)\ ),$ $D_p > 2.5$ & $D_p < 10$ µm (18b)

$V_{ds} = (d_1\ u^* + d_2\ u^{*2} + d_3\ u^{*3})\ \exp(\ (f_1\ u^* + f_2\ u^{*2} + f_3\ u^{*3})(\frac{LAI}{LAImax} -1)\ ),$ $D_p > 10$ µm (18c)

Where a_1, b_1, b_2, b_3, c_1, c_2, c_3, d_1, d_2, d_3, f_1, f_2, f_3 are coefficients defined by ZH14. LAI is the leaf area index, and LAImax its maximum value. Tables of these coefficients are given by ZH14. In our case, the c_1, c_2, c_3, f_1, f_2, f_3 coefficients are used only for deciduous broadleaf trees and long grass, while the category "short grass and forbs" is used here. According to Z01, LAI=5 for deciduous broadleaf trees, and LAImax, not given by ZH14, is set at 6.

Surface-layer parameters in GEM-AQ are calculated using Louis (1979) scheme.

b) The Brownian efficiency

Contributing to $R_{s/b}$, the Brownian efficiency E_B is, according to Z01:

$$E_B = Sc^{-\gamma} \tag{19}$$

where Sc is the Schmidt number and γ is a parameter which "*usually lies between 1/2 and 2/3 with larger values for rougher surfaces. For example, Slinn and Slinn (1980) suggested* γ*, a value of 1/2 for water surfaces. Slinn (1982) suggested* γ*, a value of 2/3 for vegetated surfaces*" [Z01]. Z01 give values of γ varying between 0.50 and 0.58 according to the land use category (LUC). P22 give a similar equation of the Brownian efficiency, based on Chamberlain [1967]:

$$E_B = \frac{Cv}{Cd} Sc^{\frac{-2}{3}} \tag{20}$$

Where C_v/C_d = 1/3 according to Chamberlain [1967]. According to PR11, MINNI uses the same formula but with C_v/C_d = 1. In summary, the models use this general formula, but with different values of both C_v/C_d and γ (Table 2):

$$E_B = \frac{Cv}{Cd} Sc^{-\gamma} \tag{21}$$

Table 2. coefficients defining the Brownian efficiency for different dry deposition parameterisations.

Models	C_v/C_d	γ
GEM_AQ, LOTOS-EUROS, IFS_Z01	1	0.50-0.58 according to the Z01 LUC
IFS_P22	1/3	2/3
MINNI	1	2/3

According to Z01, Sc depends on the kinematic viscosity of the air v, and on the particle Brownian diffusivity D_{Br}:

$$Sc = \frac{\nu}{DBr} \tag{22}$$

D_{Br} is given by KS12:

$$D_{Br} = \frac{K_{Boltzm}T}{3\,\pi\mu\,D_p} C_C \quad (23)$$

D_p is the particle diameter, T the air temperature, and μ is the dynamic viscosity of the air (kg s^{-1} m^{-1}).

For SILAM, the diffusion velocity is:

$$V_{diff} = 2\,Re^{-1/2} Sc^{-2/3} u* \quad (24)$$

Re is the canopy Reynolds number.

4 Comparison of the simulated particle dry deposition velocity to observations

This section shows the qualitative comparison between the model results and the observations compiled by P22, for the four LUC. Input data were prescribed to get intercomparable results, inspiring from previous intercomparison exercises as the Air Quality Modelling Evaluation International Initiative (AQMEII) programme [Clifton *et al.*, 2023]. Annex lists the input data and their prescribed values, as defined in the protocol, and values of some parameters specific to each model are also given, when relevant.

Figures 2 to 5 show comparisons between models and observations, for the four LUC.

4.1 Evergreen needleleaf forest

Four domains in particle diameter are defined to comment the comparison between model results and observations: D_p < 0.2 µm, where the Brownian diffusion is the main contributor to deposition, 0.2 < D_p < 2 µm, 2 < D_p < 10 µm, and D_p > 10 µm, where the sedimentation is the main contributor. A mixture of processes affect deposition in the two size domains between 0.2 and 10 um, which are mostly sedimentation and impaction. Figure 2 is commented for each size domain:

- For D_p < 0.2 µm, the model variability mainly reproduces the observation dispersion, except one observation point [observation references given by P22] above the results obtained with the parametrisation used in GEM-AQ.

- From 0.2 to 2 µm, only IFS_P22 reproduces the observed increase of V_d, compared to the smallest particles, and all other parameterisations significantly under-estimate the observation. In particular, the results obtained with the parametrisation used in SILAM are smaller than observation by 2-3 orders of magnitude, which is expected according to Kouznetsov *et al.* [2025].

- From 2 to 10 µm, the parametrisations used in LOTOS-EUROS, SILAM, MATCH and IFS_Z01 mostly underestimate the observation, while the other 5 models reproduce the observed variability.

- Above 10 µm, parameterised velocity converges to an equal value for largest particles, driven by sedimentation. Parameterised impaction generates the small spread around 10 um, which reproduce the little spread in observation. IFS_ZH14 also reproduces the averaged observation (MATCH does not provide values in this diameter range).

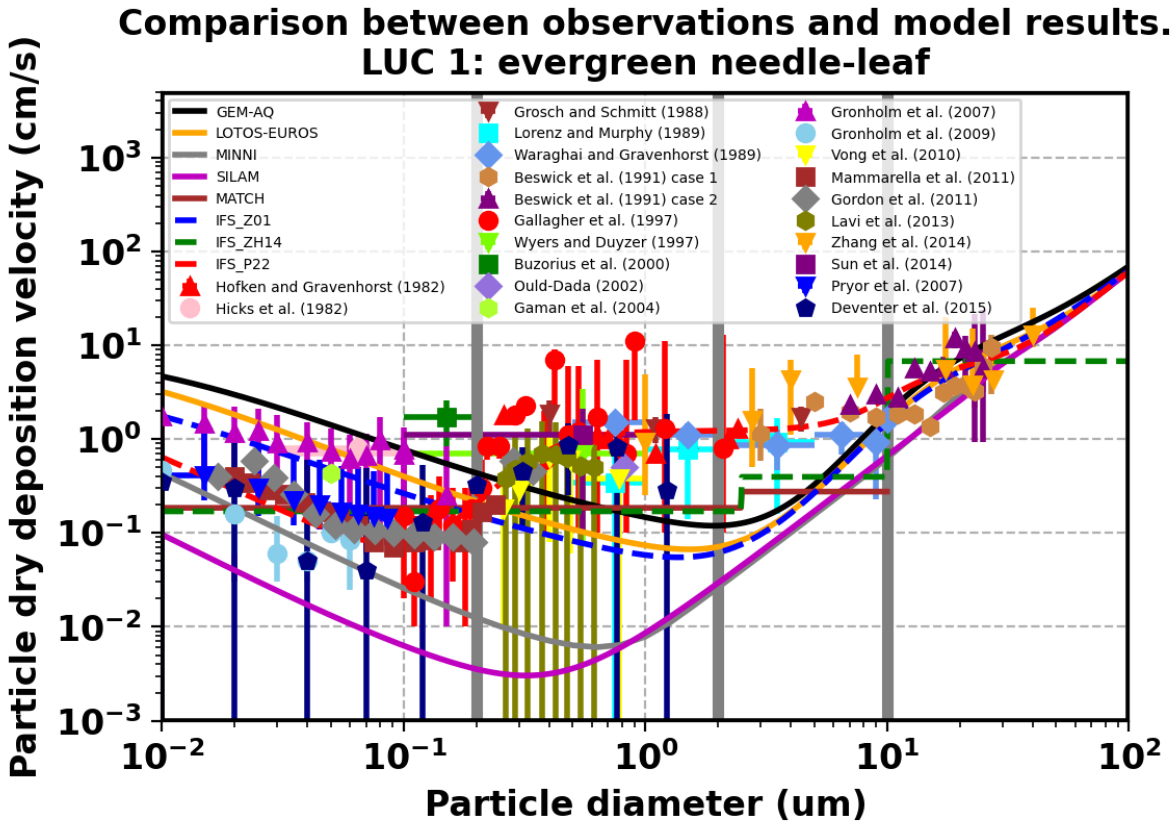

Figure 2. Comparison of the dry deposition velocity between 8 models and observation compiled by P22, for the evergreen needleleaf forest (Z01 LUC=1).

4.2 Deciduous broadleaf forest

Figure 3 shows the comparison for deciduous broadleaf forest. No observation are found with D_p > 10 µm, and a few ones above 2.5 µm, which are reproduced by the parameterisations from IFS_P22. The behaviour is similar to the evergreen needleleaf forest. In the smallest diameter interval, the observation lies within the model spread, as for the evergreen needleleaf forest, and between 0.2 and 2 µm, most models underestimate the observation, except IFS_P22.

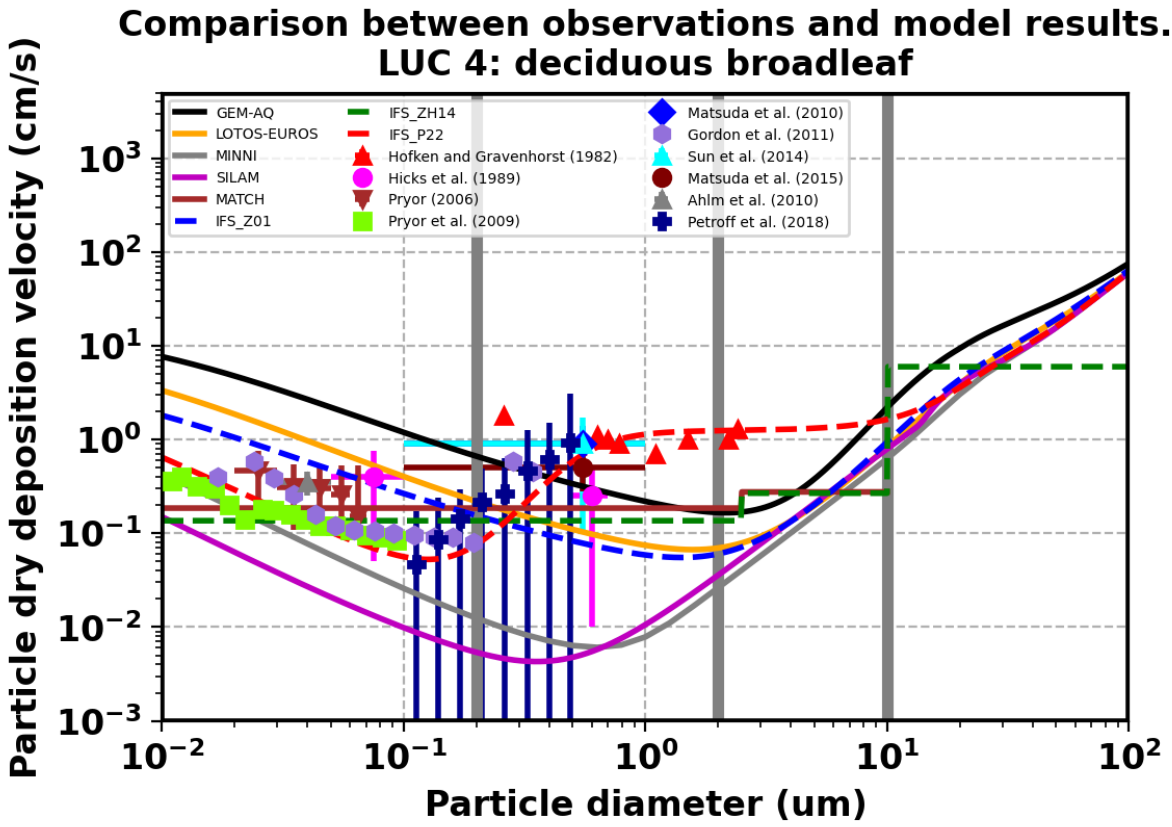

Figure 3. As Figure 2 but for deciduous broadleaf forest.

4.3 Grassland

Figure 4 shows the comparison for grass. The observation spread seems more important in grass land than in both forest categories. In particular the parameterisation implemented in SILAM are higher than observations below 0.2 µm, and other observations are significantly underestimated by all models between 0.2 and 2 µm. In the largest diameter interval, most observations lie within the model spread, except above 20 µm where some observations lie below all models.

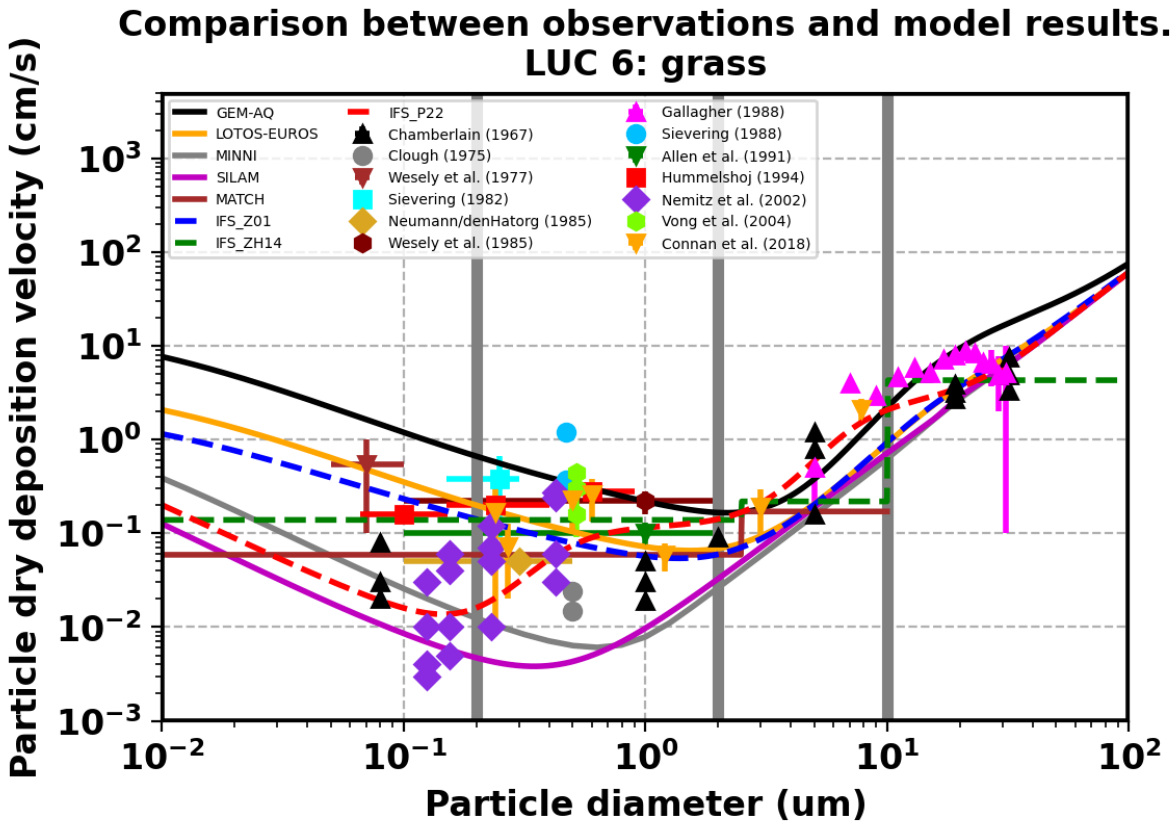

Figure 4. As Figure 2 but for grassland (Z01 land use category LUC=6).

4.4 Water

Figure 5 shows the comparison over water surfaces. Lowest values are observed over water, which are reproduced by parameterisation implemented in SILAM above 0.6 µm, and implemented in MINNI and IFS_P22 below and above 0.6 µm. However, other observations with diameter from 1 to 10 um are larger than all model results (and mostly larger than observation over other land use). Above 10 µm, all models are relatively close to observations.

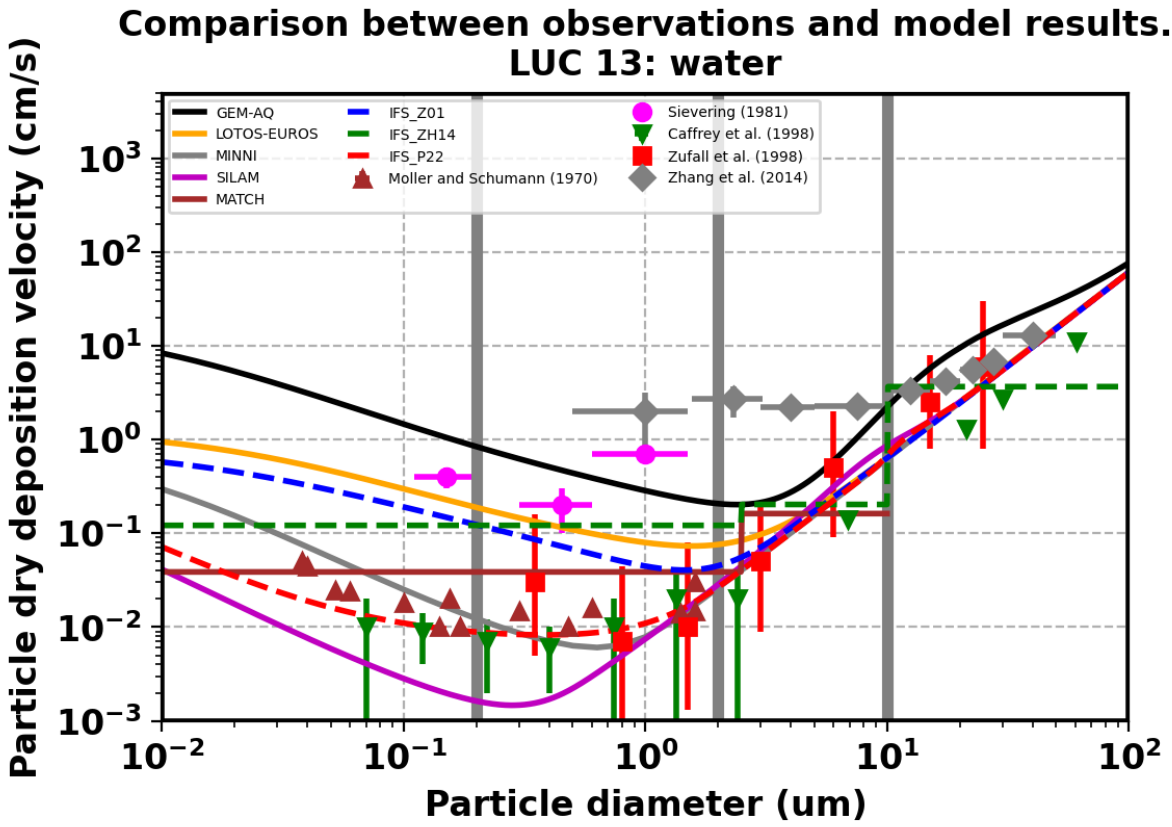

Figure 5. As Figure 2 but for water (Z01 LUC=13).

5 Comparison between models

In this Section, the focus is put on both the smallest size range and the largest size range. Brownian efficiency parameters are compared for understating the differences in the smallest size range, and the sedimentation velocity is compared for commenting the differences in the largest size range. Comparison is made for only one land use category: LUC=1, evergreen needleleaf forest.

5.1 Brownian efficiency

Figure 6 shows that the Brownian efficiency for the six parameterisation implemented in models GEM-AQ, LOTOS-EUROS, MINNI, SILAM, IFS_Z01, and IFS_P22. Neither MATCH neither IFS_ZH14 provide this component. The three modules based on Z01 closely agree: LOTOS-EUROS, GEM-AQ and IFS_Z01. The largest differences come from SILAM and IFS_P22. Indeed, the gamma parameter is 2/3 for IFS_P22 instead of 0.56 for LUC=1 by IFS_Z01. Moreover, C_v/C_d is 1/3 for IFS_P22 but 1 for the other models.

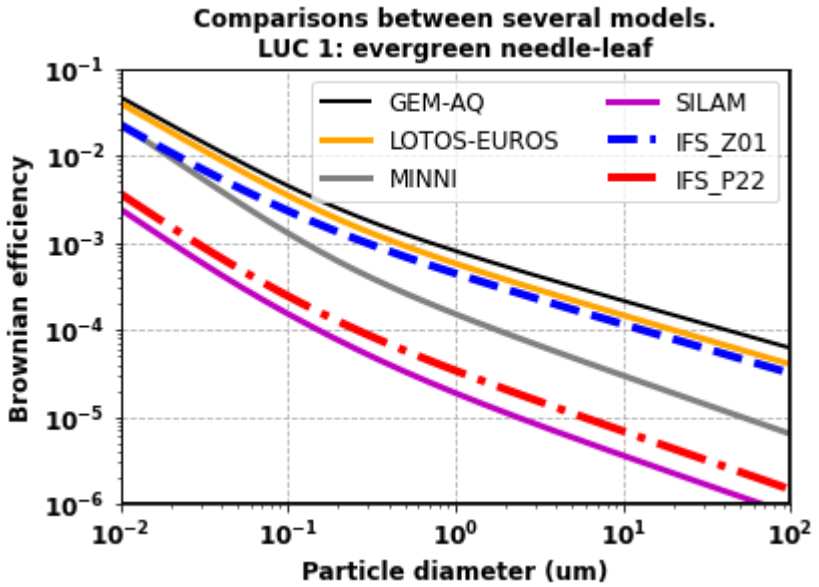

Figure 6. Comparison of the Brownian efficiency between six models, for Z01 LUC=1, which is plotted in function of the particle diameter in micrometres.

The small difference between results obtained with modules implemented in LOTOS-EUROS, on one hand, and GEM-AQ and IFS_Z01, on the other hand, originates from the Brownian diffusivity (Fig. 7). D_{Br} indeed depends on the Cunningham factor which depends on the mean free path which is around 4% larger for parameterisations from LOTOS-EUROS and SILAM than for GEM-AQ, IFS_Z01, IFS_P22 ($\lambda = 6.38\times10^{-8}$ m) (and 0.066 um according to KS12).

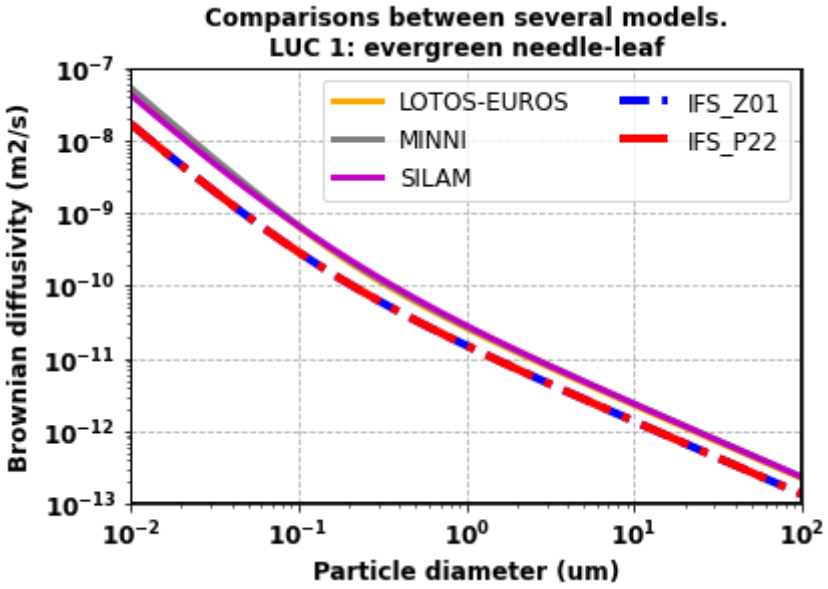

Figure 7. As Figure 6 but for the Brownian diffusivity (except no data from GEM-AQ).

5.2 The surface/quasi-laminar boundary layer resistance

The surface, or the quasi-laminar boundary layer, resistance mostly depends on the Brownian efficiency for smallest particles. And consistently with Fig. 1, the surface resistance of IFS_Z01 and the module implemented in the GEM-AQ closely agree for $D_p < 1$ µm (Fig. 8), results from LOTOS-EUROS module is slightly different because of the mean free path, and the difference is the greatest with MINNI dry deposition module and IFS_P22. For the parameterisation implemented in MINNI the difference is increased compared to the Brownian efficiency because the multiplicative factor is 1/1.2 for IFS_Z01 while it is 1/0.4 for MINNI module results. However the difference with IFS_P22 is reduced compared to the Brownian efficiency because the multiplicative factor is ½ (LAI=5).

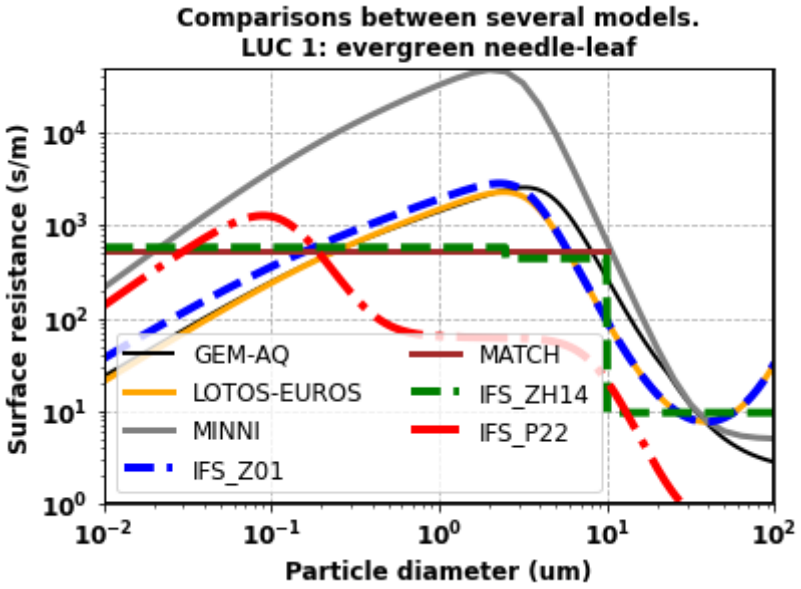

Figure 8. As Figure 6 but for the surface resistance, or the quasi-laminar boundary layer resistance, and $1/V_{ds}$ by both MATCH and IFS_ZH14 is added.

5.3 The sedimentation velocity

The sedimentation velocity is plotted for the eight models (Fig. 9). Results from six modules implemented in LOTOS-EUROS, GEM-AQ, SILAM, MINNI, IFS_Z01 and IFS_P22 agree together. IFS_ZH14 shows three steps of constant values for three diameter intervals, and MATCH shows two steps, which overall agree with these six models.

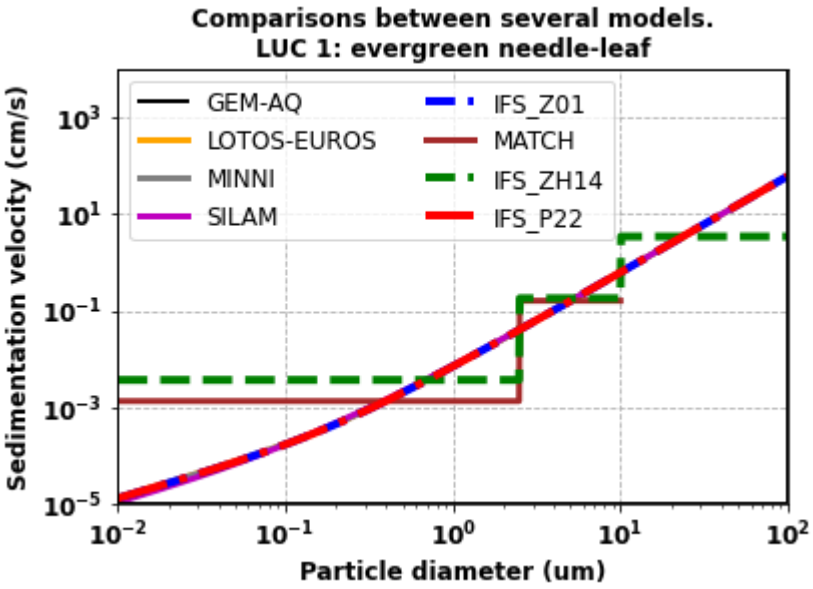

Figure 9. As Figure 6 but for the sedimentation velocity, and for the 8 modules.

6 Conclusion

Results were gathered from the 0D runs of the particle dry deposition parameterisations implemented in 5 regional models, and also from 3 modules used by IFS-COMPO. Modelled particle dry deposition velocity was plotted against particle diameter and compared to observations made over four land use categories, namely evergreen needle-leaf, water, deciduous broadleaf forest and grassland, compiled by P22. Also some other parameters were analysed to describe the variability in simulated particle dry deposition velocity, such as the Brownian efficiency and the sedimentation velocity. To acvhieve a fair comparisons between parameterisations, values of the input data (Table A1) were firstly prescribed.

Less variability according to both observation and modelling results occurs in deposition for the largest particles, which is is dominated by sedimentation. Sedimentation is modelled in more similar way between models than the other processes, for example sedimentation does not depend on the LUC, implying less variability in the results. Generally fair agreement is obtained between observation and the results from dry deposition modules in the largest range of particle size.

Significant variability is both modelled and observed in the deposition caused by Brownian diffusion for the smallest particles. It is not only dependent on LUC but also on model parameters as both the proportionality factor Cv/Cd and the exponential factor gamma defining the Brownian diffusivity. Only for grass, the observation shows values below the model range for Dp< 0.2 um, and only for evergreen needleleaf, observation shows values above the model range.

However, in comparison with observations, parameterisations mostly underestimate dry deposition velocity in the 0.2-2 µm size range, except by IFS_P22, as P22 was specifically improved compared to Z01 to reproduce these large observed values. Smallest observed values occur for water, which are reproduced by modules from SILAM, MINNI and IFS_P22.

Behaviour in the 2-10 µm follows the transition between the two adjacent size domains: over water both SILAM parameterisation and IFS_P22 reproduce closely the smallest observed values, and deposition for evergreen needleleaf and grass is quite variable according to both observation and models.

The intercomparison results suggest it could be worth testing the P22 parameterisation for particle dry deposition in future evolution of IFS_COMPO, and check its influence on arrosol fields as particle concentratioon at surface level (PM10; PM2.5), aerosol optical thickness, etc.

7 References

Chamberlain, A. C. (1967), Transport of Lycopodium Spores and Other Small Particles to Rough Surfaces, Proc. R. Soc. Ser. A, 296, 47–50.

Clifton, O. E., Schwede, D., Hogrefe, C., Bash, J. O., Bland, S., Cheung, P., Coyle, M., Emberson, L., Flemming, J., Fredj, E., Galmarini, S., Ganzeveld, L., Gazetas, O., Goded, I., Holmes, C. D., Horváth, L., Huijnen, V., Li, Q., Makar, P. A., Mammarella, I., Manca, G., Munger, J. W., Pérez-Camanyo, J. L., Pleim, J., Ran, L., San Jose, R., Silva, S. J., Staebler, R., Sun, S., Tai, A. P. K., Tas, E., Vesala, T., Weidinger, T., Wu, Z., and Zhang, L.: A single-point modeling approach for the intercomparison and evaluation of ozone dry deposition across chemical transport models (Activity 2 of AQMEII4), Atmos. Chem. Phys., 23, 9911–9961, https://doi.org/10.5194/acp-23-9911-2023, 2023.

Clifton, O. E., Schwede, D., Hogrefe, C., Bash, J. O., Bland, S., Cheung, P., Coyle, M., Emberson, L., Flemming, J., Fredj, E., Galmarini, S., Ganzeveld, L., Gazetas, O., Goded, I., Holmes, C. D., Horváth, L., Huijnen, V., Li, Q., Makar, P. A., Mammarella, I., Manca, G., Munger, J. W., Pérez-Camanyo, J. L., Pleim, J., Ran, L., San Jose, R., Silva, S. J., Staebler, R., Sun, S., Tai, A. P. K., Tas, E., Vesala, T., Weidinger, T., Wu, Z., and Zhang, L.: A single-point modeling approach for the intercomparison and evaluation of ozone dry deposition across chemical transport models (Activity 2 of AQMEII4), Atmos. Chem. Phys., 23, 9911–9961, https://doi.org/10.5194/acp-23-9911-2023, 2023.

Farmer, D. K., Boedicker, E. K., and DeBolt, H. M., Dry Deposition of Atmospheric Aerosols: Approaches, Observations, and Mechanisms, Annu. Rev. Phys. Chem. 2021. 72:375–97, https://doi.org/10.1146/annurev-physchem-090519-034936.

Kouznetsov, R., and M. Sofiev (2012), A methodology for evaluation of vertical dispersion and dry deposition of atmospheric aerosols, J. Geophys. Res., 117, D01202, doi:10.1029/2011JD016366

Kouznetsov, R., Sofiev, M., Uppstu, A., and Hänninen, R.: Deposition velocity concept does not apply to fluxes of ambient aerosols, EGUsphere [preprint], https://doi.org/10.5194/egusphere-2025-2364, 2025.

Mailler, S., Menut, L., Cholakian, A., and Pennel, R.: AerSett v1.0: a simple and straightforward model for the settling speed of big spherical atmospheric aerosols, Geosci. Model Dev., 16, 1119–1127, https://doi.org/10.5194/gmd-16-1119-2023, 2023.

Pleim, J., and L. Ran (2011), Surface flux modeling for air quality applications, Atmosphere, 2(3), 271–302, doi:10.3390/atmos2030271.

Pleim, J. E., Ran, L., Saylor, R. D., Willison, J., & Binkowski, F. S. (2022). A new aerosol dry deposition model for air quality and climate modeling. *Journal of Advances in Modeling Earth Systems*, *14*, e2022MS003050

Simpson, D., Benedictow, A., Berge, H., Bergström, R., Emberson, L. D., Fagerli, H., Flechard, C. R., Hayman, G. D., Gauss, M., Jonson, J. E., Jenkin, M. E., Nyíri, A., Richter, C., Semeena, V. S., Tsyro, S., Tuovinen, J.-P., Valdebenito, Á., and Wind, P.: The EMEP MSC-W chemical transport model – technical description, Atmos. Chem. Phys., 12, 7825–7865, https://doi.org/10.5194/acp-12-7825-2012, 2012.

Seinfeld, J., and S. Pandis (2006), Atmospheric Chemistry and Physics, 2nd ed., 1225 pp., John Wiley, Hoboken, N. J.

Slinn, W. G. N. (1982), Predictions for particle deposition to vegetative canopies, Atmos. Environ., 16(7), 1785–1794, doi:10.1016/0004-6981(82), 90271-2.

Wesely, M. L., Cook, D. R., Hart, R. L., and Speer, R. E.: Measurements and Parameterization of Particulate Sulfur Dry Deposition over Grass, J. Geophys. Res., 90, 2131–2143, 1985.

Zhang, L., Gong, S., Padro, J., Barrie, L. (2001). A size-segregated particle dry deposition scheme for an atmospheric aerosol module. *Atmospheric Environment*, *35*(3), 549–560. https://doi.org/10.1016/s1352-2310(00)00326-5

Zhang, L. and He, Z.: Technical Note: An empirical algorithm estimating dry deposition velocity of fine, coarse and giant particles, Atmos. Chem. Phys., 14, 3729–3737, https://doi.org/10.5194/acp-14-3729-2014, 2014.

8 Annex

We list here the required values of most parameters, for the intercomparison exercise (Table A1). Moreover we give some parameters specific to each model:

- Computations by GEM-AQ are made for a stability function of 0, giving an aerodynamic resistance of 14.9 s/m.

- Computations by MINNI are made in the configuration of w*=0.

- Computations by SILAM are made for 1/L=0, L being the Monin-Obukhov length, which defines the atmospheric stratification.

- For MATCH, the Monin-Obukhov length L affects the stability function (psiH) which affects the aerodynamic resistance. L is 1000 here, providing Ra=20.9 s/m for evergreen needleleaf, with psiH=-0.12. For L < 0, V_{ds} also includes an enhancement factor of 3 for fine nitrate particles, which is not included here as L > 0.

- For deciduous broadleaf forest by ZH14, LAImax is set at 6.

- for water surface by IFS_P22, the water surface temperature is 15°C, and the wind speed at 10 m above the surface is 10 m/s. The white cap fraction is then included between 1 and 2%. Contrarily to P22, LAI is fixed at 1 in order to avoid an infinite value of the quasi-liminar layer resistance.

Table A1. List of input parameters and prescribed values for the comparison exercise (the values to be used are shown in **bold**). For the friction velocity, the roughness length, the leaf area index, and the characteristic radius, four values are given for the four LUC: evergreen needleleaf (LUC = 1 according to Z01, 4 according to ZH14, group 2), deciduous broadleaf (4, 7, group 2), grassland (6, 13-14, groups 4-3), water (13-14, 1, 3, group 5). Following the season classification by Z01, SC1 is chosen, for "midsummer, with lush vegetation".

parameter	Parameter label	Unit	Also listed by Clifton *et al.* [2023]	Values in Z01	Values in P22	**Our study**
Particle diameter	D_p	µm				**From 0.01 to 100 µm, 1000 steps in logarithmic scale**
Air pressure	P_a	Pa	x			**101 325**
Air temperature	T_a	°C	x			**15**
Friction velocity	U*	m/s	x		0.4, 0.4, 0.3, 0.2	**0.4, 0.4, 0.3, 0.2**
Roughness length	Z0	M	x	0.80, 1.05, 0.10, f(u)		**0.80, 1.05, 0.10, 0.001**
Computation height	Zr	M	x	20		**20**
Air density	r_{air}	kg/m^3	x			**1.225**
Particle density	r_p	kg/m^3		2000		**2000**
Leaf area index	LAI	m^2/m^2	x	/	5, 5, 2, 0	**5, 5, 2, 0**
Characteristic radius for Z01	A	Mm		2, 5, 2, /	/	**2, 5, 2, *I***
Von Karman constant	κ	None				**0.4**
Gamma for the Brownian diffusivity		None		0.56, 0.56, 0.54, 0.50	2/3	

Document History

Version	Author(s)	Date	Changes
1.0	Thierry Elias and Samuel Rémy	17/06/2025	Initial version
1.1	Thierry Elias and Samuel Rémy	26/06/2025	Revised according to the internal reviews

Internal Review History

Internal Reviewers	Date	Comments
Joanna Struzewska	19/06/2025	
Jeronimo Escribano	20/06/2025	